The 2013 World Congress on
Advances in Structural Engineering and Mechanics (ASEM13)
Jeju, Korea, September 8-12, 2013

Behaviour of concrete-filled steel tubular column to restrained steel beam joints after exposed to full-range fire

*Tian-Yi Song[1)], Lin-Hai Han[2)], Zhong Tao[3)]

[1,) 3)] *Institute for Infrastructure Engineering, University of Western Sydney, Penrith NSW 2751, Australia*
[2)] *Department of Civil Engineering, Tsinghua University, Beijing, 100084, China*
[1)] *t.song@uws.edu.au*

ABSTRACT

Numerical analysis is performed to investigate the behaviour of concrete-filled steel tubular (CFST) column to restrained steel beam joints after exposed to full-range fire with initial load. Based on a validated finite element analysis (FEA) model, failure mode, deformations, internal force and moment of the CFST column to axially and rotationally restrained steel beam joint in the ambient loading, heating, cooling and post-fire phases are analysed. Finally, the joint moment versus relative rotation angle curve of this type of composite joint in the full-range phase is analysed, which can be used to evaluate the post-fire behaviour of the joint in the further research.

Key words: Concrete filled steel tubular (CFST); Steel beam; Joint; Finite element analysis; Full-range analysis

1. INTRODUCTION

Concrete filled steel tubular (CFST) columns have been used widely in the construction of new buildings due to their excellent structural performance. The CFST column to steel beam joint with external rings as a type of typical beam-column rigid joint has been adopted in many high-rise buildings in recent years. However, limited research has been done to investigate the performance of CFST column to steel beam joints after fire (Han et al. 2012).

For a real structure subjected to fire, the structural components generally experience an entire time (t) - temperature (T) - load (N) path, as shown in Fig. 1, which includes: 1) ambient loading phase (AA'). Apply initial load (N_o) on the structural component at ambient temperature; 2) Heating phase (A'B'). Increase environmental temperature and keep N_o constant; 3) Cooling phase (B'C'D'). After environmental temperature achieves T_h corresponding to the heating time (t_h), the temperature starts

[1)] Doctor
[2)] Professor
[3)] Associate Professor

to decrease with constant load N_o, where, t_p and t_d represent the times that environmental and structural temperature drop to ambient temperature, respectively; 4) Post-fire loading phase ($D'D_p$). After the structural temperature drops to ambient temperature, increase external load until the structural component fails at critical load (N_{cr}).

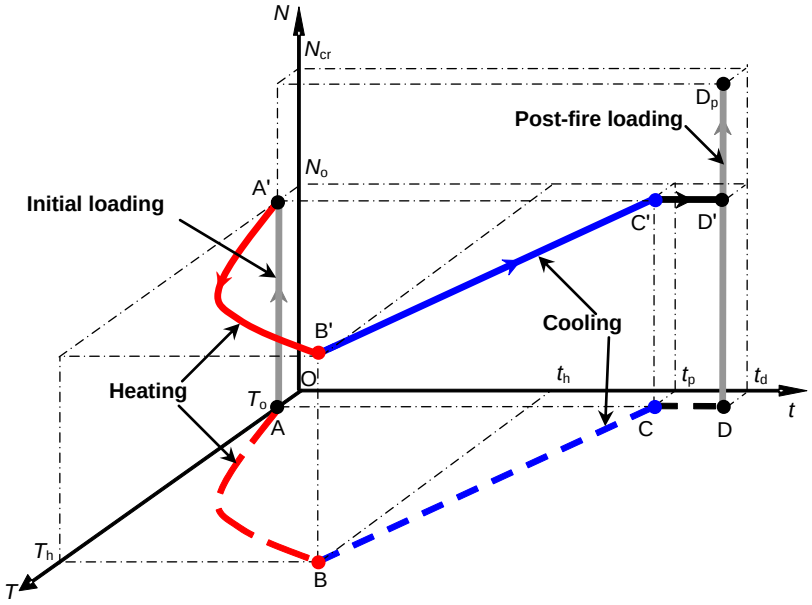

Fig. 1 Time (t) - temperature (T) - load (N) path

The significant influence of the full-range A-A'-B'-C'-D'-D_p path, as shown in Fig. 1, on the post-fire performance of structures has been identified by the studies on CFST columns (Yang et al. 2008; Song et al. 2010b). But for CFST column to steel beam joints with external rings, the research based on A-A'-B'-C'-D'-D_p path is very limited. Song et al. (2010a) conducted tests on CFST column to unrestrained steel beam joint specimens under the full-range A-A'-B'-C'-D'-D_p path, and a finite element analysis (FEA) model was established to simulate the joint tests.

However, for joints in real structures, the beam ends of a joint are generally restrained by the adjacent components. Therefore, the research on joints should consider the influence of restrained steel beams to reflect the real situation. In this paper, the FEA model proposed by Song et al. (2010a) is further developed to simulate the CFST column to axially and rotationally restrained steel beam joint isolated from a CFST planar frame. A full-range analysis is performed to understand the response of this type of composite joints under the entire load and fire phase.

2. ESTABLISHMENT OF THE FINITE ELEMENT ANALYSIS MODEL

The sequentially-coupled thermal-mechanical analysis module in ABAQUS software is adopted to establish the FEA model of CFST column to restrained steel beam joints.

2.1 General description of the FEA model

The cruciform beam-column joint isolated from a planar frame is chosen as the

calculation model. The joint is composed of a circular CFST column, two steel beams connected with the column through external rings and a reinforced concrete (RC) slab connected with the steel beam via shear connectors. The vertical load (N_F) and uniform load (q) are applied on the column and RC slab, respectively. The ends of the beam and slab are restrained against rotations and translation in the axial direction, the bottom of the column is fixed, and the top of the column is restrained against rotations. The part of the joint under the RC slab exposes to ISO-834 (1980) heating and cooling fire.

In the modelling, a typical CFST to restrained steel beam joint with the RC slab is designed according to standards DBJ 13-51-2003 (2003) and GB 50017-2003 (2003). Fire protection insulation is applied on the surfaces of the CFST column and steel beam to satisfy the fire resistance requirement in standard GB 50016-2006 (2006). Dimensions of the joint are shown in Table 1, where D_c is the outside diameter of the circular CFST column section; t_s is the thickness of the steel tube; H is the height of the column; h and b_f are the height and width of the steel beam respectively; t_w and t_f are the thickness of the web and thickness of the flanges of the steel beam respectively; L is the length of the steel beam; b_{slab} and t_{slab} are the width and thickness of the slab; L_{slab} is the length of the slab. The longitudinal and distribution bars in the RC slab are φ10@150mm and φ10@250mm, respectively. The width of the external rings is 120mm. φ16×100mm shear connectors are configured in two rows along the beam with the spacing of 200mm.

Table 1 Dimensions of the CFST column to restrained steel beam joint

CFST column (mm)			H-shaped steel beam (mm)			RC slab (mm)	
$D_c \times t_s$	H	a_c	$h \times b_f \times t_w \times t_f$	L	a_b	$b_{slab} \times t_{slab}$	L_{slab}
600×12	6000	15	400×200×15×15	8000	20	3000×120	8000

For the material properties, the strength of core concrete in the CFST column (f_{cuc}) is 60 MPa; the strength of concrete in the RC slab (f_{cus}) is 40 MPa; the yield strength of the steel tube (f_{yc}) and that of the steel beam (f_{yb}) are 345 MPa; the yield strength of the steel bars in the RC slab (f_{ybs}) is 335 MPa; the tensile strength of the shear connectors is 400 MPa.

For the load and fire conditions: the column's load ratio ($n=N_F/N_u$) is 0.6, where N_u is the axial compressive capacity of the column at ambient temperature; the beam's load ratio ($m=q/q_u$) is 0.4, where q_u is the ultimate capacity of the composite beam under uniform load; the heating time ratio ($t_o=t_h/t_r$) is 0.5, where t_h is the heating time, and t_r is the fire resistance of the joint.

Based on the above calculation conditions, the temperature field analysis model and mechanical analysis model were developed. For the temperature field analysis model, the modelling method proposed by Song et al. (2010a) was adopted. The effect of heat convection and radiation were considered in the temperature field analysis. For the mechanical analysis model, the material properties of steel and concrete at ambient,

heating, cooling and post-fire phases, element types and methods for simulating the core concrete-steel tube interface and the steel bar-concrete interface suggested by Song et al. (2010a) were adopted. Fig. 2 illustrates the element division, thermal and mechanics boundary conditions of the joint model.

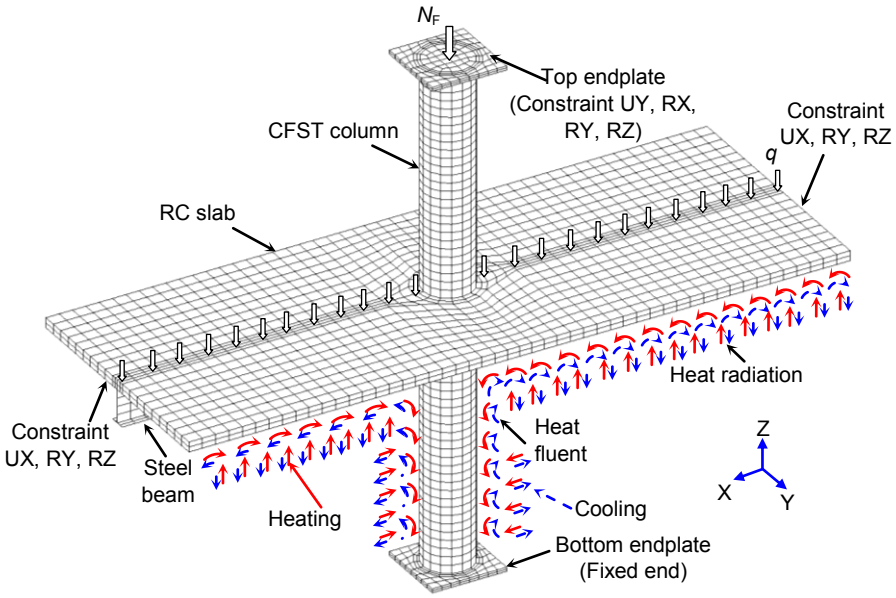

Fig. 2 Element division and boundary conditions of the CFST column to restrained steel beam joint

In the FEA model, the slippage between the steel beam and RC slab and the steel high-temperature creep were considered. For the slippage between the steel beam and RC slab, two-node spring elements were used to simulate the relative slippage. To capture the interface behavior, a shear force (Q)–relative slippage (δ) relation as a function of temperature need to be input into the spring elements. However, there is no such model available, which needs further research. In this paper, a Q–δ equation for shear connectors at ambient temperature proposed by Ollgaard et al. (1971) was tentatively adopted with modified ultimate shear bearing capacity corresponding to different temperatures according to EN 1994-1-2: 2005 (2005). The steel high-temperature creep strain equation suggested by Fields and Fields (1991) was embedded into the User subroutine "UEXPAN" in ABAQUS software to consider the effect of the steel high-temperature creep in the steel tube and steel beam. Details can be found in Song (2011).

2.2 Validation of the FEA model

Due to the absence of experiments on circular CFST column to restrained steel beam joints with external rings after exposed to full-range fire, the fire and post-fire test data on circular CFST columns and CFST column to unrestrained steel beam joints with external rings reported by previous researchers (Han 2007; Lie and Chabot 1992; Huo et al. 2010; Han et al. 2007; Song et al. 2010a) are used to verify the FEA model indirectly. The comparison between predicted and tested results demonstrates the

accuracy of the FEA model. In this paper, only the comparison with the post-fire joint tests conducted by Huo et al. (2010) and Han et al. (2007) is presented.

Huo et al. (2010) and Han et al. (2007) conducted cyclic tests on six circular CFST column to steel beam joint specimens with external rings after exposed to ISO-834 standard fire. During the testing, the joint specimens were exposed to ISO-834 fire without applying any external load first. After the specimens were heated to the predetermined heating time, the specimens were cooled to ambient conditions. When the specimen temperature dropped to ambient temperature, the joint specimens were assembled on the testing machine, and a horizontal cyclic load was applied on the column to investigate the post-fire cyclic behaviour of this type of joints.

Fig. 3 shows the comparison between the predicted and measured post-fire lateral load (P) versus lateral deformation (Δ) envelope curves. It can be seen that the accuracy of FEA model is acceptable.

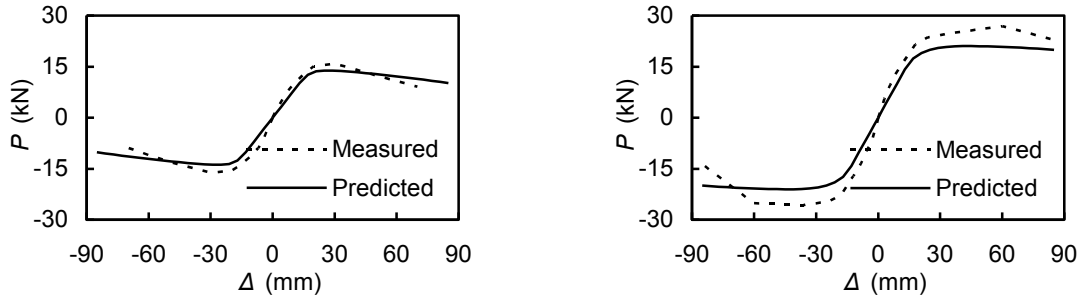

(a) Specimen C11 (Han et al. 2007) (b) Specimen C23 (Huo et al. 2010)

Fig. 3 Comparison between predicted and measured P-Δ envelope curves

Fig. 4 shows the observed and predicted failure modes of the specimen C11, where "S" in Fig. 4(b) represents the Mises stress of the steel tube and beam. The predicted result indicates that the web and flanges of the steel beam near the external rings develop the maximum Mises stress, and local bucking occurs in these regions, which is consistent with the observed result.

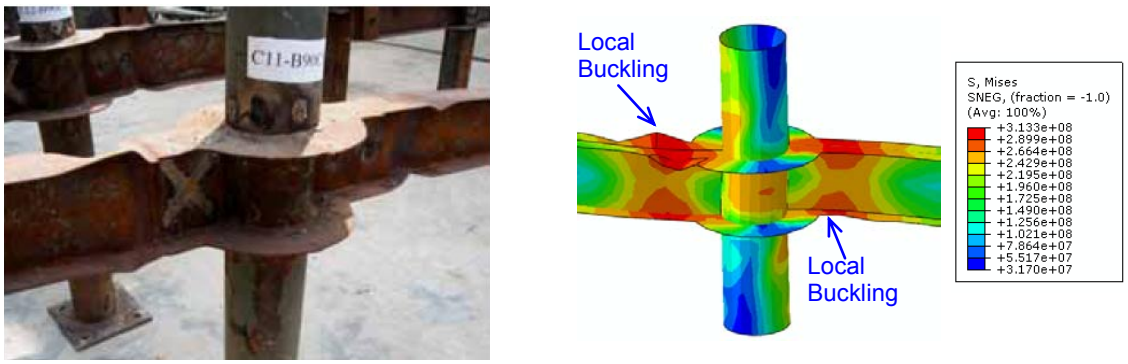

(a) Observed (Han et al. 2007) (b) Predicted

Fig. 4 Comparison between predicted and observed failure mode

Based on the verified FEA model, the full-range analysis on CFST column to restrained steel beam joints subjected to full-range fire is performed in the following.

3. FULL-RANGE MECHANICAL ANALYSIS

The performance of CFST column to restrained steel beam joints in the full-range loading and fire phase is studied in this Section.

3.1 Failure mode

In the entire loading and fire phases, the joint may fail in different phases, such as, failure at ambient loading phase due to the increased external load; failure at heating or cooling phases due to the degraded material properties and changed internal forces. The failure occurred at the heating phase is also named as fire resistance of the joint. In this paper, the research will focus on the case of joint failure occurred in the post-fire phase.

Fig. 5 shows the typical failure mode of the CFST column to restrained steel beam joint after exposed to heating and cooling fire. It can be found that the CFST column shows good working performance, no significant deformation or steel tube local buckling is observed. The joint fails due to the local buckling of the bottom flange and web of the steel beam in the joint zone.

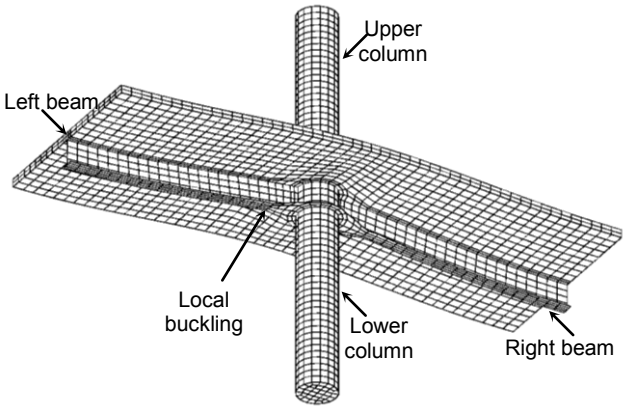

Fig. 5 Failure appearance of the CFST column to restrained steel beam joint

3.2 Deformation development

Deformations of the composite joint, including axial deformation of the column, deflection of the beam and relative rotation angle between the column and beam, are calculated and analysed. The definition of the axial deformation of the column (Δ_c) and deflection of the beam (δ_b) are illustrated in Fig. 6.

For the relative rotation angle between the column and beam (θ_r), the definition proposed by Mao et al. (2010) is adopted, which is:

$$\theta_r = \theta_c - \theta_b = \tan^{-1}[(\Delta_{c1} - \Delta_{c2})/ h_c] - \tan^{-1}[(\Delta_{a1} - \Delta_{b1})/ h_1] \quad (1)$$

where Δ_{a1}, Δ_{b1}, Δ_{c1} and Δ_{c2} represent the horizontal displacement of the intersection points A_1, B_1, C_1 and C_2, respectively. h_1 and h_2 represent the distance between A_1 and B_1, C_1 and C_2, respectively. The position of points A_1, B_1, C_1 and C_2 are shown in Fig. 6.

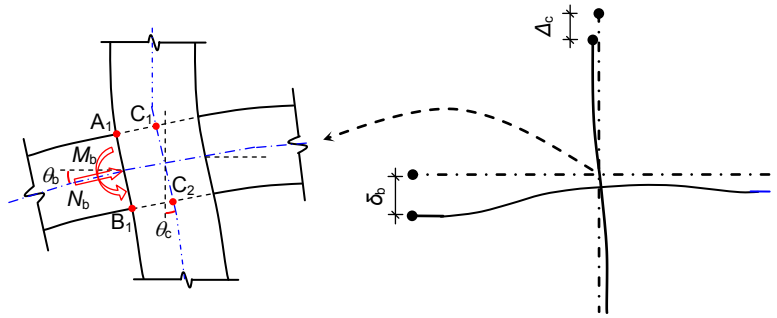

Fig. 6 Definition of joint deformations and internal forces

The axial deformation of the column (Δ_c) and beam end deflection (δ_b) versus time (t) curves in the entire loading and fire phase are illustrated in Figs. 7(a) and (b) respectively, in which, points A, A', B', C' and D' correspond to the points in Fig. 1, and point E' represents the ending of post-fire loading.

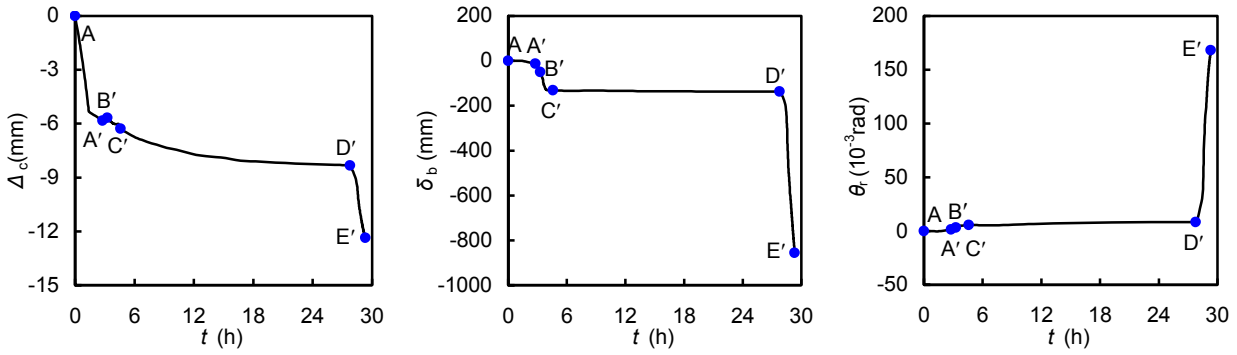

(a) Δ_c - t curve (b) δ_b - t curve (c) θ_r - t curve

Fig. 7 Deformations of the joint in the entire phase

For the axial deformation of the column in Fig. 7(a), in the ambient temperature phase (AA'), axial contraction of the column keeps increasing as the increasing of the load on the column and the beam. In the heating phase (A'B'), axial expansion of the column can be observed due to the thermal expansion. In the cooling phase (B'C'D'), it takes about 1.5h for the fire temperature drops to ambient temperature at point C', but for the temperature inside the joint, it takes more than 20h to drop to ambient temperature. Comparing with the column axial deformation occurred at B'C' phase, the axial deformation occurred at C'D' phase is more significant. It is attributed to the contraction of material in the cooling phase. After the joint temperature drops to normal temperature (D'E'), the column's axial contraction increases as the increasing of beam load.

It can be seen from Fig. 7(b) that the deformation of the beam is greater than the deformation of the column. At the end of the heating phase, the beam's deflection is about -50 mm, and at the end of the cooling phase, the beam's deflection reaches up to -140 mm. The increment of the beam's deflection in the cooling phase is about 2.3 times of the increment of the beam's deflection in the heating phase, which means the joint in the cooling phase is more dangerous compared with the joint in the heating phase due to the significant beam's deformation. In the post-fire phase, the beam's deflection increases as the increasing of the beam load until the joint fails.

Fig. 7(c) illustrate the relative rotation angle between the column and beam (θ_r) of the joint versus time (t) curve, in which, positive and negative relative rotation angels represent that the angels between the column and beam are less and greater than 90 angle, respectively. It can be concluded that, in the ambient temperature phase (AA'), θ_r increases as the increasing of the external load applied on the column and beam, and it reaches about 1.45×10^{-3} rad. In the heating and cooling phases (A'B'C'D'), θ_r keeps increasing as the increasing of time, but the increment is moderate. That means the working ability of this type of external ring connection is good at high temperature condition. In the post-fire phase (D'E'), θ_r increases as the increasing of the beam's load until the joint fails.

3.3 Internal axial force and moment of the beam

The internal axial force (N_b) and internal moment (M_b) of the beam, as shown in Fig. 6, are calculated. The N_b versus time (t) and M_b versus t curves are shown in Fig. 8.

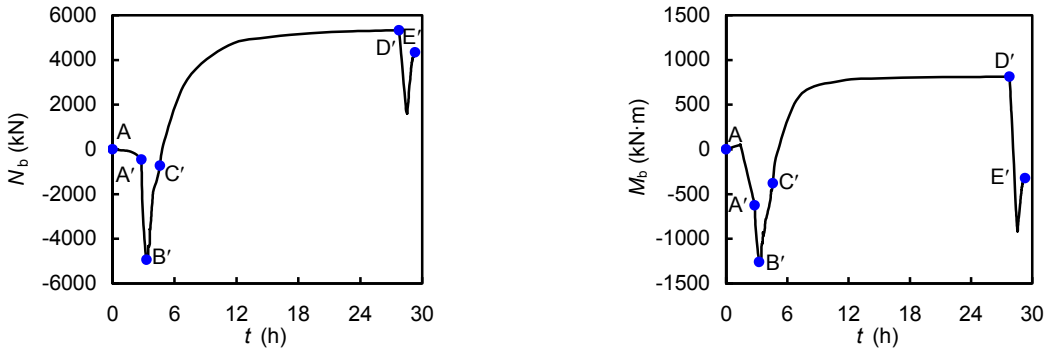

(a) N_b - t curve (b) M_b - t curve

Fig. 8 Internal axial force (N_b) and moment (M_b) of beam in joint zone

For the internal axial force, a negative axial force represents that the beam is in compression, and a positive axial force represents the beam is in tension. It can be found from Fig. 8 (a) that, in the ambient temperature phase (AA'), as the increasing of the external loads on the column and beam. The axial compressive force of the beam reaches about -450 kN due to the restrained axial deformation. Then in the heating phase (A'B') the axial compressive force raises up to -4900 kN due to the fact that thermal expansion of the beam in the axial direction is restrained. In the cooling phase (B'C'D'), the axial force of the beam varies from -4900 kN to +5000 kN due to the restrained axial contraction as the decreasing of the temperature. In the post-fire phase

(D'E'), as the increasing of the load on the beam, the internal axial tensile force in the beam decreases first and then increases. For the internal moment, a negative moment represents the top of the beam is in tension and the bottom of the beam is in compression, whilst a positive moment represents the opposite situation. It can be found from Fig. 8(b) that the external load on the beam and the heating fire tend to increase the negative moment of the beam in the joint zone, but the cooling fire tends to increase the positive moment of the beam.

4. JOINT MOMENT VERSUS RELATIVE ROTATION ANGLE CURVE

The joint residual strength and residual stiffness are two important parameters which can be used to assess the post-fire performance of the CFST column to restrained steel beam joint after exposed to a full-range fire. The two parameters can be determined from the joint moment (M) versus relative rotation angle (θ_r) curve. Therefore, in this paper, the M - θ_r curve of the joint during the entire loading and fire phase is calculated and illustrated in Fig. 9, where, M is equal to M_b, as shown in Fig. 6.

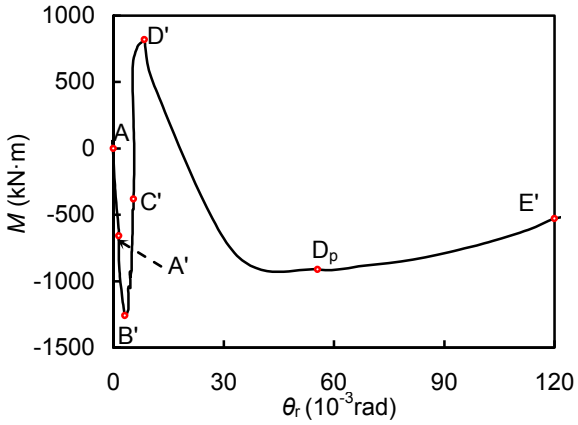

Fig. 9 Joint moment (M) versus relative rotation angle (θ_r) relation

From Fig. 9, the following observations may be made regarding the M–θ_r curve of the joint with an initial load subjected to heating and cooling fire:

(1) In the ambient loading phase (AA'): With the increasing of the external loads, the negative joint moment increases as the increasing of the relative rotation angle.

(2) In the heating phase (A'B'): The negative joint moment keeps increasing as the increasing of the relative rotation angle. The absolute value of the tangent slope at A' point in the A'B' curve is slightly greater than that in the AA' curve. It can be explained by the influence of the compressive axial force in the beam as mentioned before.

(3) In the cooling phase (B'C'D'): The joint moment changes from negative to positive due to the influence of restrained thermal deformation in the beam, and the relative rotation angle increases moderately.

(4) In the post-fire phase (D'D_pE'): After the joint temperature drops to ambient temperature, the column's load remains stable, but the uniformly distributed load on the beam increases until the joint fails. It can be found that the negative moment keeps

increasing as the relative rotation angle increases until reaching point D_p, and then the negative moment starts to decrease. It indicates that the joint reaches its ultimate state at point D_p, because the joint cannot bear any more external load after this point, and the negative moment corresponding to point D_p can be designated as the post-fire ultimate bending capacity of the joint.

Based on the $M–\theta_r$ curve, the joint residual strength and stiffness can be defined and calculated in the further research.

5. CONCLUSIONS

A FEA model of a CFST column to restrained steel beam joint was built to analyse the behavior of the joint after exposed to full-range fire with an initial load. Based on the FEA model, mechanics characteristics of the joint, including failure mode, deformations, internal force and moment of the beam, were predicted and discussed. Finally, the joint moment versus relative rotation angle curve was drawn to investigate the response of the joint during the entire load and fire phase, which can be used to evaluate the post-fire residual joint strength and stiffness in the further research.

6. ACKNOWLEDGEMENTS

This research was supported by China National Key Basic Research Special Funds project under Grant No. 2012CB719700. The Project was also supported by the Australian Research Council (ARC) under its Discovery Projects scheme (Project No: DP120100971). The financial support is highly appreciated.

REFERENCES

DBJ13-51-2003. (2003), *Technical specification for concrete-filled steel tubular structures*, China (Fujian): Fujian Local Standard in Engineering Construction (in Chinese).

EN 1994-1-2:2005. (2005), *Design of composite steel and concrete structures-part1-2: General rules-structural fire design*, European Committee for Standardization, Brussels.

Fields, B.A. and Fields, R.J. (1991), *The prediction of elevated temperature deformation of structural steel under anisothermal conditions*, National Institute of Standards and Technology, Gaithersburg, MD, NCSTIR 4497.

GB50017-2003. (2003), *Code for design of steel structures*, Beijing: China Planning Press (in Chinese).

GB50016-2006. (2006), *Code of design on building fire protection and prevention*, Beijing: China Planning Press (in Chinese).

Han, L.H. (2007), *Concrete filled steel tubular structures - theory and practice. 2nd ed*, Beijing: Science Press (in Chinese).

Han, L.H., Huo, J.S. and Wang, Y.C. (2007), “Behavior of steel beam to concrete-filled steel tubular column connections after exposure to fire”, *J. Struct. Eng., ASCE,* Vol. 133(6), 800-814.

Han, L.H., Song, T.Y. and Tan, Q.H. (2012), “Fire performance of steel-concrete composite structures in China: Test, analysis and design approach”, *10th International Conference on Advances in Steel Concrete Composite and Hybrid Structures*, Singapore.

Huo, J.S., Han, L.H. and Wang, Y.C. (2010), “Behaviour of repaired concrete filled steel tubular column to steel beam joints after exposure to fire”, *Adv. Struct. Eng.,* Vol. 13(1), 53-67.

ISO-834. (1980), *Fire-resistance tests-elements of building construction*, International Standard ISO834: Amendment 1, Amendment 2.

Lie, T.T. and Chabot, M. (1992), *Experimental studies on the fire resistance of hollow steel columns filled with plain concrete*, Ottawa, Canada: NRC-CNRC Internal Report. No.611.

Mao, C.J., Chiou, Y.J., Hsiao, P.A. and Ho, M.C. (2010), “The stiffness estimation of steel semi-rigid beam–column moment connections in a fire”, *J. Constr. Steel. Res.,* Vol. 66(5), 611-736.

Ollgaard, J.G. Slutter, R.G. and Fisher, J.W. (1971), “Shear strength of stud connectors in lightweight and normal-weight concrete”, *AISC Eng. J.*, 1971: Vol. 8(2), 55-64.

Song, T.Y. (2011), *Research on post-fire performance of steel-concrete composite beam-column joints*, Beijing: Tsinghua University (in Chinese).

Song, T.Y., Han, L.H. and Uy, B. (2010a), “Performance of CFST column to steel beam joints subjected to simulated fire including the cooling phase”, *J. Constr. Steel. Res.,* Vol. 66(4), 591-604.

Song, T.Y., Han, L.H. and Yu, H.X. (2010b), “Concrete filled steel tube stub columns under combined temperature and loading”, *J. Constr. Steel. Res.,* Vol. 66(3), 369-384.

Yang, H., Han, L.H. and Wang, Y.C. (2008), “Effects of heating and loading histories on post-fire cooling behaviour of concrete-filled steel tubular columns”, *J. Constr. Steel. Res.,* Vol. 64(5), 556-570.